

# Restoration, seismic strengthening and seismic design for railway viaducts after Hyogoken-Nanbu Earthquake

Nobuyuki Matsumoto <sup>a,\*</sup>, Yukio Kitago <sup>b</sup>, Tsutomu Sato <sup>a</sup>

<sup>a</sup> *Structure Technology Development Division, Railway Technical Research Institute, 2-8-38 Hikari-cho, Kokubunji-shi, Tokyo, Japan*

<sup>b</sup> *Engineering Department, JR West Japan Consultants Company, 5-4-20 Nishinakajima, Yodogawa-ku, Osaka, Japan*

---

## Abstract

Numbers of railway viaducts were severely damaged and collapsed in the Hyogoken-Nanbu Earthquake in January 1995. Intensive restoration works were conducted to make early re-operation of the damaged railway lines. An urgent strengthening operation was put in motion to provide sufficient shear strength and ductility for existing RC viaduct columns. Most of the restoration works and strengthening operation were conducted using the steel jacketing method. New seismic strengthening methods using synthetic materials, such as carbon, aramid and glass fibers, have been proposed and also applied. After a lapse of four years, a draft of new seismic design specification for railway structures was proposed. In this article, the outlines of restoration of damaged structures in the Hyogoken-Nanbu Earthquake, design methods and their research backgrounds of new strengthening method, and the concept of new seismic design standards will be presented. © 2000 Elsevier Science Ltd. All rights reserved.

**Keywords:** Railway structure; Concrete structure; Rigid frame viaduct; Restoration; Seismic strengthening; Seismic design; Shear strength; Ductility; Synthetic material

---

## 1. Introduction

The Hyogoken-Nanbu Earthquake occurred on 17 January 1995 at 5:46 a.m. caused catastrophic damages not only to buildings and highway structures but also to railway structures.

Eight units of reinforced concrete viaducts were totally collapsed in Sanyo Shinkansen Line and many other RC viaducts in commuter railway lines, such as the JR West Tokaido Trunk Line, Hankyu, Hanshin, Kobe Express, Sanyo and Kobe City Railway Lines, were also suffered collapse and severe damages. Intensive restoration works on damaged structures were conducted and this led to the early re-operations of the most of these railway lines. Extensive strengthening operations have been also conducted on existing RC viaducts, whose columns were judged to have insufficient shear strengths, primarily using steel jacketing method. After a lapse of four years, those strengthening operations for the Shinkansen networks were finished and for other trunk lines have been almost finishing. Within these years, a lot of new strengthening methods

using synthetic materials have been proposed and made practicable. A draft of new seismic design specifications was also proposed.

## 2. Restoration works

### 2.1. Structure of viaduct and characteristics of damage

The structure of viaduct which is commonly used in Japanese railway companies is the reinforced concrete rigid frame composed of beams, slab floor and columns as shown in Fig. 1. It is called *rahmen* viaduct. When the Sanyo Shinkansen Line was constructed, a standardized or predetermined design was applied to accomplish rapid construction. Then, the beams and the slabs of the viaducts are designed rigidly not to change their dimensions even when the height of columns are varied.

The damaged parts of viaducts were then primarily concentrated to their column members. As the columns or vertical members were destroyed, the falling or subsidence of beams and slabs or superstructures occurred. The damages of superstructures, however, were relatively light.

---

\* Corresponding author.

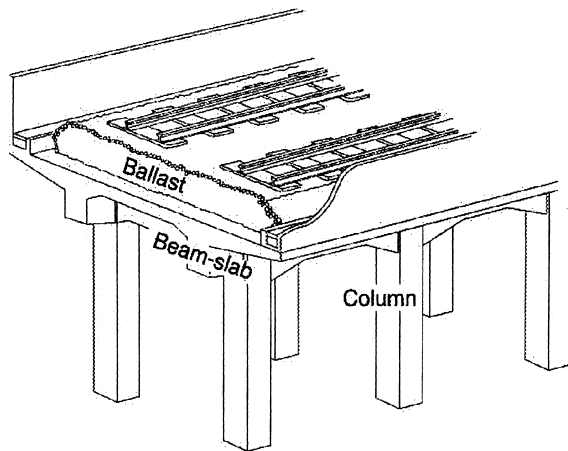


Fig. 1. Schematics of rigid frame viaduct.

## 2.2. Concept of restoration works

Through the damage inspection of viaducts, it was found that the damage of superstructures (beams and slabs) were negligible so these members were reused as much as possible. On the other hand, most of the vertical members or columns were damaged and should be restored or rehabilitated. Restoration methods to increase the ductility of columns were mainly used. They were selected to avoid bad influences on the foundation piles. The fundamental concept of restoration works were common for the Shinkansen lines and the commuter trunk lines.

## 2.3. Details of restoration works on rigid frame viaducts

The damages of viaducts were classified into three categories based on their appearances as shown in Table 1. The schematics of these classified damages and their restoration methods are shown in Figs. 2–4.

As the restoration method for the Type-I damaged columns, the grouting of concrete cracks with epoxy resin was first conducted and then the steel jacket retrofitting was applied. The gap between steel jacket and existing column was grouted with shrinkage-compensating mortar.

For the Type-II damaged columns, which have little subsidence of beams and slabs, additional hoops of 13 mm diameter (D13) spaced at 100 mm were first arranged around the damaged sections and steel jacket plates with 6–9 mm thickness were placed to encase the whole length of columns. The gap between steel jacket and existing concrete column was grouted with shrinkage-compensating mortar. The grouting of concrete cracks with epoxy resin was conducted after steel jacketing and mortar grouting.

The restoration method for the Type-III damaged columns is as follows. The slabs and beams are temporarily supported by steel assemblies. Then, the damaged columns are taken away from the beam–column joints leaving a short length of longitudinal reinforcing bars of columns stuck out from the joints. The separated slabs and beams were jacked up to the original height. New longitudinal reinforcing bars for columns were welded to ones extended from beam–column joints and from footings by the gas-pressure welding method [1]. These new longitudinal reinforcing bars were spliced and welded at the middle section of the column. Hoops using the D13 reinforcing bar spaced at 100 mm were provided. Then, steel jacket of 6–9 mm thickness was placed to encase the columns. Shrinkage-compensating mortar was grouted in the steel jacket.

As for the gas-pressure welding, the hot shearing method, which removes flash immediately after welding with a shearing edge, was adopted. Using this method, visual inspections are easily possible to check welding defects for all the welded reinforcing bars.

When a set of upper slab and beam (deck) could not be lifted at once by jacks because of their capacities, the deck was cut and separated. The longitudinal reinforcing bars stuck out from the separated beams were also welded using the hot-shearing gas-pressure welding method to new reinforcing bars in order to extend their lengths. Then, the extended reinforcing bars were spliced and welded each other. At the welded section, stirrups of D16 reinforcing bars spaced at 100 mm are provided. The original longitudinal reinforcing bars were cold-work bent and straightened, therefore extra longitudinal reinforcing bars were placed at the splice section to

Table 1  
Classification of damages

| Type of damage | Extent of damage | Explanation of damage  | Approximate number of damaged columns |
|----------------|------------------|--|---------------------------------------|
| Type-I         | Moderate         | Cracks were formed. Moderately damaged. See Fig. 2.  | 1200                                  |
| Type-II        | Severe           | Spalling of cover concrete were observed but the subsidence of beams and slabs are small. Severely damaged. See Fig. 3.                                | 1200                                  |
| Type-III       | Collapsed        | Crush of concrete and bent, buckling or rupture of reinforcing bar was observed. The subsidence of beams and slabs are obvious. Collapsed. See Fig. 4. | 1000                                  |

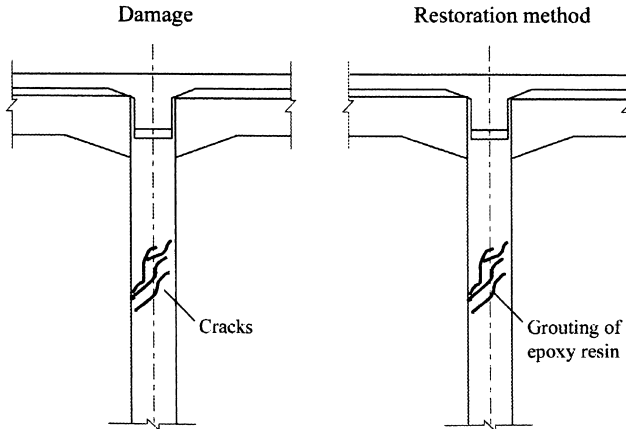


Fig. 2. Type-I damage and restoration method.

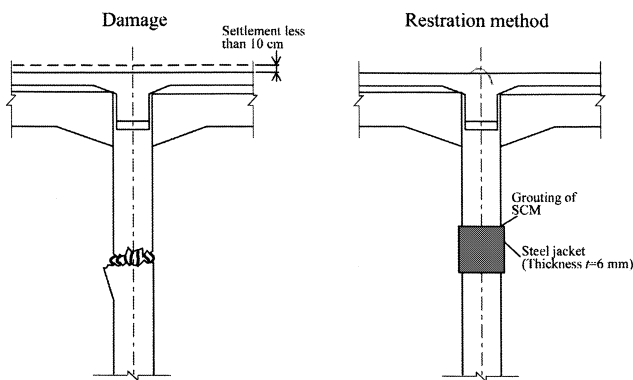


Fig. 3. Type-II damage and restoration method.

avoid the decrease of fatigue capacity. Furthermore, steel plates of 6 mm thickness were attached on the concrete surface at the section.

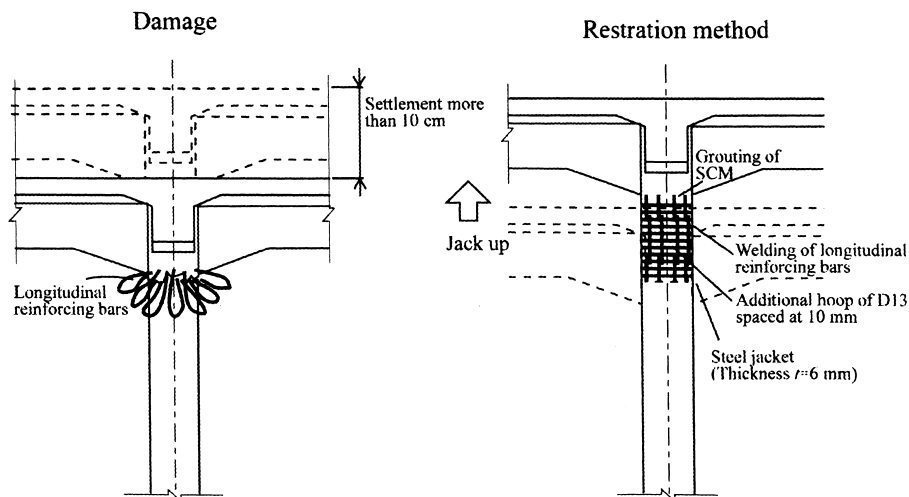


Fig. 4. Type-III damage and restoration method.

#### 2.4. Evaluation of materials in damaged structures and ductility of restored structures

Some of the reinforcing bars were taken out from the damaged columns and evaluated whether they were suitable to be reused. Their strengths are shown in Fig. 5. It was revealed that all the specimens satisfied the nominal yield strength, ultimate strength and elongation requirement, so they are reused in the restoration works.

On the other hand, cyclic loading tests were conducted using scale-modeled columns of existing viaducts and of steel jacket strengthened. It was obtained that the ductility factor  $\mu$  of nonstrengthened column was 2 and that of steel jacket strengthened column was approximately 10. Then, it was evaluated that the equivalent elastic horizontal seismic coefficient for the strengthened column increased two and a half times that of non-strengthened one.

### 3. Strengthening methods for existing railway viaducts

#### 3.1. Target of seismic strengthening

The investigation on the causes of damages of structures during the Hyogoken-Nanbu Earthquake and the necessity of seismic strengthening for existing railway structures were discussed in the Railway Facilities Seismic Structure Investigation Committee which was organized by the Ministry of Transportation right after the earthquake. A notification of urgent seismic strengthening [2] was issued in July 1995 to execute necessary strengthening on the existing railway structures. For the RC viaducts, the numbers of columns as shown in Table 2 were selected for strengthening.

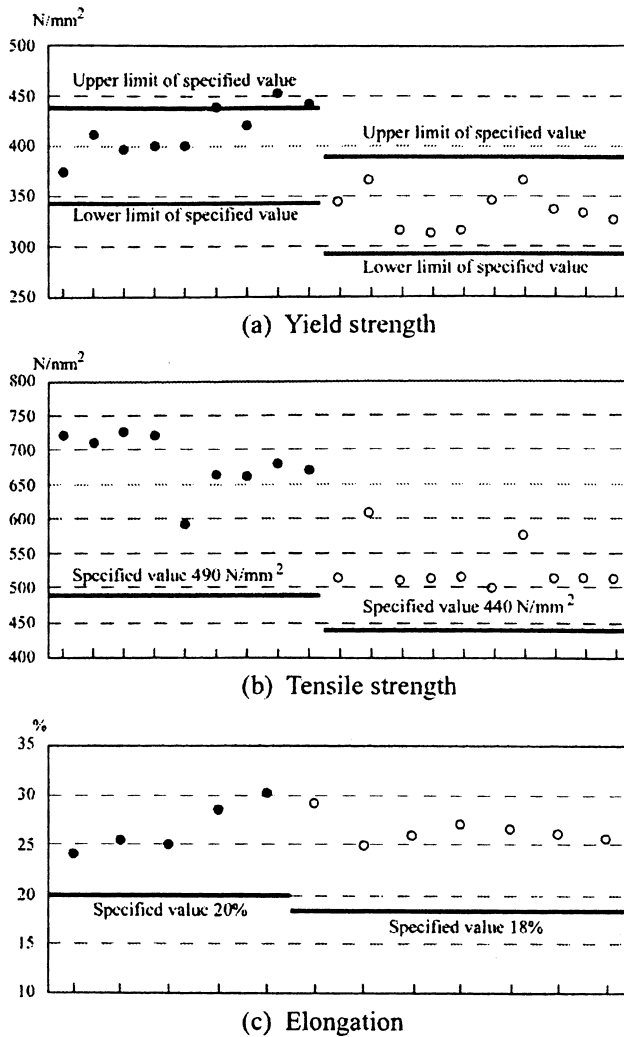


Fig. 5. Strength and elongation of reinforcing bars from damaged structures.

Table 2  
Numbers of RC viaduct columns selected for urgent seismic strengthening

|                                    | Duration (yr) | Numbers |
|------------------------------------|---------------|---------|
| JR                                 |               |         |
| Shinkansen lines                   | 3             | 25 000  |
| Trunk lines                        | 5             | 8000    |
| Private sector lines, Subway lines | 5             | 13 000  |
| Total                              | —             | 46 000  |

Columns which have the shear failure mode (shear failure occurs before plastic hinge forms) or do not have sufficient ductility against expected earthquake were selected. The intensity of Hyogoken-Nanbu Earthquake was taken into account for the expected earthquake.

Required performances for the seismic strengthening methods for railway RC structures were the abilities to prevent shear failure and improve ductility of members.

### 3.2. Seismic strengthening methods and strengthening performance evaluation

Various kinds of seismic strengthening methods had been studied before and after the Hyogoken-Nanbu Earthquake to satisfy the above-mentioned required performances. Among them, strengthening methods which neither change the structural system of viaduct nor impose excessive loads to foundation piles were chosen as practical seismic strengthening methods for railway RC viaduct columns. Design guidelines for these seismic strengthening methods, as shown in Table 3, were documented in the format of limit state design method. Cyclic loading tests using full size or close to full size specimens were conducted to confirm the performances of these strengthening methods. The ductility of strengthened members was obtained by these experiments. The ductility factor for the strengthened member was defined as shown in Fig. 6. This is the same definition as the one used in the Design Standards for Railway RC Structures [3].

The finite element analysis was also used to evaluate shear capacities of new strengthening methods. Outline of practical strengthening method used in railway RC viaduct and their seismic performances are as follows.

#### 3.2.1. Steel jacketing

Steel jacketing is the most popular strengthening method for railway RC viaduct columns in Japan. Six to 12 mm thick rectangular steel plates are placed around the existing RC column and the gap between steel plates and existing column is grouted with shrinkage-compensated mortar or epoxy resin as shown in Fig. 7.

The shear capacity of concrete member strengthened by steel jacketing is calculated according to an evaluation equation for composite structure as shown in Eq. (2) in Table 4. The ductility of steel jacketed member is

Table 3  
Seismic strengthening methods of which design guidelines were made

| Strengthening methods          |
|--------------------------------|
| Steel jacketing method         |
| Carbon fiber wrapping method   |
| Aramid fiber wrapping method   |
| Steel cloth wrapping method    |
| GFRP shotcreting method        |
| Concrete jacketing method      |
| Shotcreting method             |
| Spiral wire wrapping method    |
| Precast panel jacketing method |

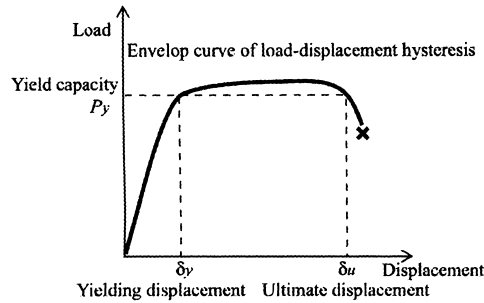


Fig. 6. Definition of ductility factor ( $\mu = \delta_u/\delta_y$ ). Yielding disp.: displacement at yielding of longitudinal reinforcement. Ultimate disp.: maximum displacement to keep the yielding capacity on the envelope curve of hysteresis.

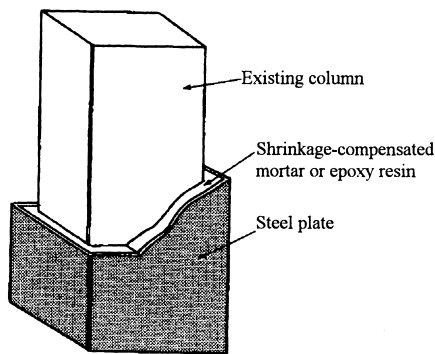


Fig. 7. Steel jacketing method.

evaluated using Eqs. (3) and (4) based on several experimental results.

The steel plates were welded to close their joints until the restoration work of Hyogoken-Nanbu Earthquake. New mechanical joints as shown in Fig. 8 were proposed for the seismic strengthening.

### 3.2.2. Fiber sheet wrapping

Fiber sheet wrapping method uses epoxy resin impregnated carbon or aramid fiber sheets. They are affixed on the surface of existing columns as shown in Fig. 9. As for carbon fiber sheet, the tensile strength of 2500–4500 MPa and the elastic modulus of 235 GPa is generally used. As for aramid fiber sheet, the tensile strength of 2500–3500 MPa and the elastic modulus of 120 or 80 GPa is generally used [4,5].

Shear tests were conducted using  $60 \times 60 \text{ cm}^2$  square section specimens. Analyses using the finite element method were also conducted and one of their results is shown in Fig. 10. Through these studies, it was observed that the shear capacity of fiber sheet strengthened member increases in proportion to the amount of fiber sheet while the capacity is governed by the rupture of fiber sheet. Then, the shear capacities provided

by fiber sheets were evaluated using the modified truss analogy procedure. It was revealed that the shear capacities provided by fiber sheet do not reach to the full strength predicted by the modified truss analogy. So, modification factors to reduce the strengthened capacities were introduced. They were taken as 0.8 and 0.4 for carbon and aramid fiber sheets, respectively.

It was also observed that there is little shear strengthening effect when the amount of fiber sheet is very small because of the rupture of sheet due to local large deformation produced by shear cracks. On the other hand, the failure mode changes from the rupture of fiber sheet to the compression failure of concrete when the amount of fiber sheet exceeds a certain value. The practical range of the amount of fiber sheet required for the shear strengthening of railway viaduct column is approximately within the range of which the rupture of fiber sheet occurs. Then, Eq. (7) is proposed for the design shear strength evaluation.

Cyclic loading tests were conducted to evaluate the ductility of fiber sheet strengthened members. The deformation ductility factor was evaluated in relation to the moment–shear capacity ratio ( $V_{yd}l_a/M_{ud}$ ) as shown in Fig. 11. The test results were linearly approximated. The lower limit lines were used as the design equations as shown in Eqs. (8) and (9).

### 3.2.3. GFRP shotcreting

GFRP shotcrete strengthening method uses admixture of short glass fibers and polyester resin. It is sprayed as shown in Fig. 12 to the surface of existing RC member. The tensile strength of hardened GFRP shotcrete and its elastic modulus are 80 MPa and 7.5 GPa, respectively, when the fiber content ratio is approximately 35%.

The shear capacity of GFRP shotcrete strengthening was also evaluated using the modified truss analogy and the design equation was derived as Eq. (11). The design equation for ductility factor was also derived using the results of cyclic loading tests as Eq. (12) under the specified conditions on capacity ratios  $V_{GFd}/V_{Mud}$  and  $V_{GFyd}/V_{Mud}$ .

### 3.2.4. Concrete jacketing, shotcreting and precast panel jacketing

Several kinds of concrete-based strengthening methods were developed. The concrete jacketing, shotcreting and precast panel jacketing are shown in Figs. 13–15, respectively. The shear capacity and ductility factor of strengthened member are evaluated assuming it behaves like a monolithic member. They are calculated according to the design equations in the Design Standards for Railway Concrete Structures.

Table 4  
Shear capacities and ductilities evaluated in design guidelines for railway structures

| Strengthening methods  | Shear capacities   | Ductility factors   |
|--|--|---|
| <i>Jacketing or wrapping with steel or synthetic materials</i> |  |   |
| Steel jacketing  | $V_{\text{Sjyd}} = V_{\text{cd}} + V_{\text{sd}} + V_{\text{Sjd}}$   | (1) $\mu_{\text{Sjd}} = \frac{\mu_{\text{OSj}}\delta_{y0} + \delta_{u1}}{\delta_{y0} + \delta_{y1}} \leq 10$ (3)    |
|  | $V_{\text{Sjyd}}$ : design strengthened shear capacity   | (4) $\mu_{\text{OSj}} = -1.6 + 6.6 \frac{V_{\text{Sjyd}} l_a}{M_u} + 11.2 p_{\text{wSj}}$                           |
|  | $V_{\text{cd}}$ : shear capacity provided by concrete  | $\mu_{\text{Sjd}}$ : design strengthened ductility factor   |
|  | $V_{\text{sd}}$ : shear capacity provided by shear reinforcement   | $\mu_{\text{OSj}}$ : ductility factor of member without hinge area  |
|  | $V_{\text{Sjd}}$ : shear capacity provided by steel jacket   | $\delta_{y0}$ : displacement due to member at yielding  |
|  | $V_{\text{Sjd}} = \frac{f_{\text{ryd}} z_w t_w}{\gamma_b}$   | (2) $\delta_{y1}$ : rotational displacement due to pull-out of longitudinal reinforcement at yielding               |
|  | $f_{\text{ryd}}$ : shear yield strength of steel plate ( $f_{\text{ryd}}/\sqrt{3}$ )   | $\delta_{u1}$ : rotational displacement due to pull-out of longitudinal reinforcement at ultimate stage             |
|  | $z_w$ : web height of steel plate  | $V_{\text{r}}$ : Shear capacity of existing member  |
|  | $t_w$ : web thickness of steel plate   | $l_a$ : shear span, $M_u$ : moment capacity of existing member  |
|  | $\gamma_{\text{bsj}}$ : member factor (1.0)  | (5) $p_{\text{wSj}}$ : reinforcing ratio, $p_{\text{wSj}} = \frac{2t + (A_b/s)}{b}$                                 |
| Carbon or aramid fiber sheet wrapping                          | $V_{\text{FSyd}} = V_{\text{cd}} + V_{\text{sd}} + V_{\text{FSd}}$   | (6) Carbon fiber sheet:   |
|  | $V_{\text{FSyd}}$ : design strengthened shear capacity   | $\mu_{\text{CFd}} = 2.8 + 1.15 \frac{V_{\text{CFyd}} l_a}{M_{\text{CFud}}} \leq 10$ (8)                             |
|  | $V_{\text{FSyd}}$ : design shear capacity provided by carbon fiber sheet   | $\mu_{\text{CFd}}$ : design strengthened ductility factor   |
|  | $V_{\text{FSd}} = K \frac{A_{\text{FS}}/f_{\text{FSud}} (\sin \alpha_{\text{FS}} + \cos \alpha_{\text{FS}})}{S_{\text{FS}}} \frac{z}{\gamma_{\text{bFS}}}$ | (7) $V_{\text{CFyd}}$ : design strengthened shear capacity  |
|  | $K$ : correction factor for fiber sheet (Carbon: 0.8, Aramid: 0.4)   | $M_{\text{CFud}}$ : design strengthened moment capacity   |
|  | $A_{\text{FS}}$ : area of fiber sheet within a distance $S_{\text{FS}}$ and with an angle of $\alpha_{\text{FS}}$  | Aramid fiber sheet:   |
|  | $f_{\text{FSud}}$ : design tensile strength of fiber sheet   | (9) $\mu_{\text{AFd}} = 2.2 + 3.2 \frac{V_{\text{AFyd}} l_a}{M_{\text{AFud}}} \leq 10$                              |
|  | $\alpha_{\text{FS}}$ : angle between fiber sheet and longitudinal axis of member (rad)   | $\mu_{\text{AFd}}$ : design strengthened ductility factor   |
|  | $S_{\text{FS}}$ : unit width of fiber sheet  | $V_{\text{AFyd}}$ : design strengthened shear capacity  |
|  | $\gamma_{\text{bFS}}$ : member factor (1.15)   | $M_{\text{AFud}}$ : design strengthened moment capacity   |
|  | $z$ : distance from acting position of compressive stress resultant to centroid of tension reinforcement   |   |
| GFRP shotcreting   | $V_{\text{GFyd}} = V_{\text{cd}} + V_{\text{sd}} + V_{\text{GFd}}$   | (10) $\mu_{\text{GFd}} = \frac{(0.72(l_a/d) + 0.44)(l_a/100)}{\delta_y} \frac{1}{\gamma_{\text{bGF}}} \leq 10$ (12) |

|   |   |
|---|---|
| $V_{GFyd}$ : design strengthened shear capacity<br>$V_{GFd}$ : design shear capacity provided by GFRP   | $\mu_{GFd}$ : design strengthened ductility factor<br>d: effective depth  |
| $V_{GFd} = \frac{A_{GF} f_{GFud} (\sin \alpha_{GF} + \cos \alpha_{GF})}{S_{GF}} \frac{z}{\gamma_{bGF}}$ | (11) $\delta_y$ : yielding displacement   |
| $A_{GF}$ : area of GFRP within a distance of $S_{GF}$ and with an angle of $\alpha_{GF}$                | $\gamma_{bGF}$ : member factor (1.3)  |
| $f_{GFud}$ : design tensile strength of GFRP  | where, $V_{GFd}/V_{Mud} \geq 1.0$ and $V_{GFyd}/V_{Mud} \geq 1.5$   |
| $\alpha_{GF}$ : angle between GFRP and longitudinal axis of member (rad)                                | $V_{Mud}$ : design shear force when bending moment reaches to the bending capacity of member  |
| $S_{GF}$ : unit width of GFRP, $\gamma_{bGF}$ : member factor (1.15)                                    |   |
| <i>Concrete or concrete base material jacketing</i>   |   |
| Concrete jacketing  | $\mu_d = \frac{\mu_0 \delta_{y0} + \delta_{ud}}{\delta_{y0} + \delta_{y1}}$ (14)  |
|   | $\mu_0 = -1.6 + 5.6 \frac{V_{sd} L_u}{M_{ud}} + (11.4 p_s - 1.4) p_s$ (15)  |
| Shotcreting   | $\mu_d$ : design strengthened ductility factor  |
| Spiral wire wrapping  | $\mu_0$ : ductility factor of member without hinge area   |
| Precast panel jacketing   | $\delta_{y0}$ : displacement due to member at yielding<br>$\delta_{y1}$ : rotational displacement due to pull-out of longitudinal reinforcement at yielding<br>$\delta_{ud}$ : rotational displacement due to pull-out of longitudinal reinforcement at ultimate stage<br>$\delta_{yd}$ : design shear capacity<br>$p_s$ : shear reinforcement ratio<br>$M_{ud}$ : design moment capacity |

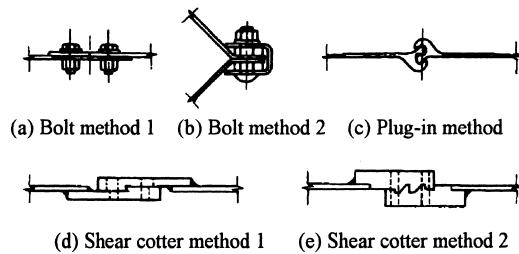


Fig. 8. New joint method for steel jacking.

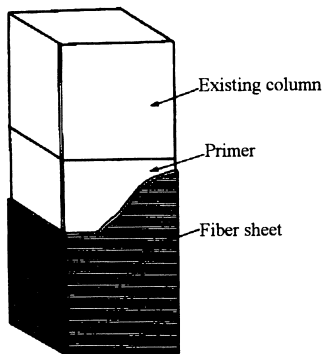


Fig. 9. Synthetic sheet wrapping.

Shear stress carried by fiber sheet  $\tau$  (MPa)

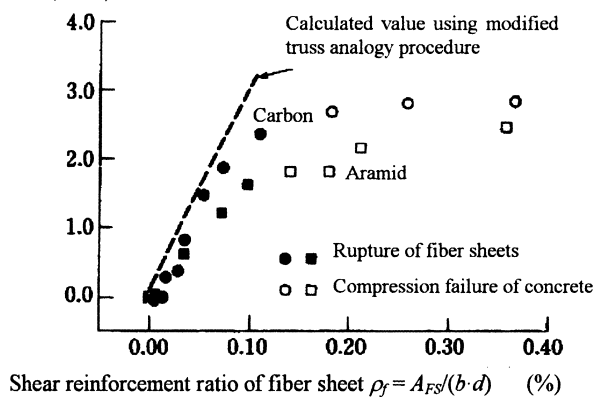


Fig. 10. Shear stress carried by fiber sheet.

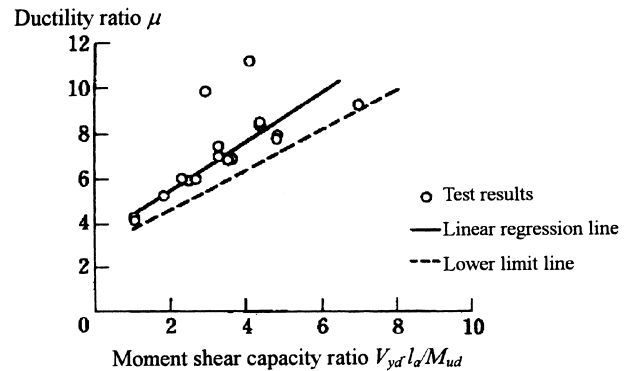


Fig. 11. Ductility of carbon fiber sheet wrapping.

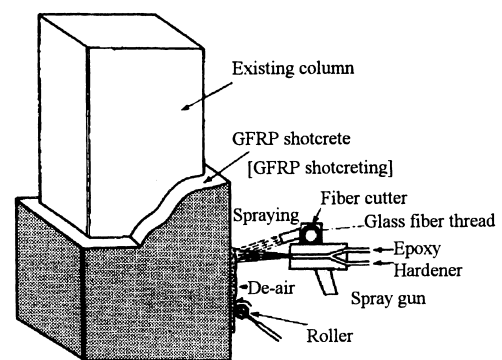


Fig. 12. GFRP shotcreting.

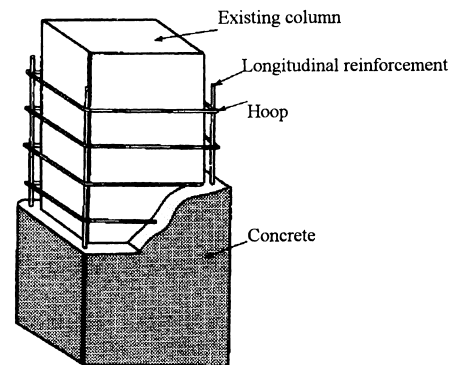


Fig. 13. Concrete jacking.

## 4. New seismic design

### 4.1. Introduction

After 4-year investigations and studies on the characteristics of Hyogoken-Nanbu Earthquake and damages of structures, a final draft of New Seismic Design for Railway Structures [6] was proposed in December 1998 by a subcommittee of the Railway Facilities Seismic Structure Investigation Committee taking into account the concept of performance base design.

### 4.2. Design assumed earthquake

Two levels of earthquake motions, which are defined depending on the probability of occurrence during the design lifetime of structure as shown in Table 5, are taken into account in the new design standards.

Level-1 (L1) Earthquake Motion is determined by a seismic risk analysis for earthquakes which have the return period of 50 yr. The design response spectrum is shown in Figs. 16–18. The maximum acceleration response spectrum value is  $250 \text{ cm/s}^2$ .



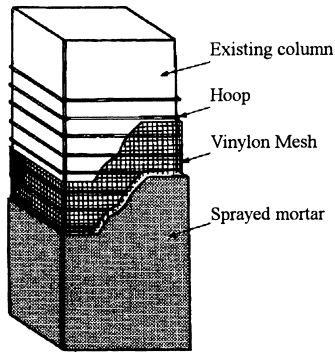


Fig. 14. Shotcreting.

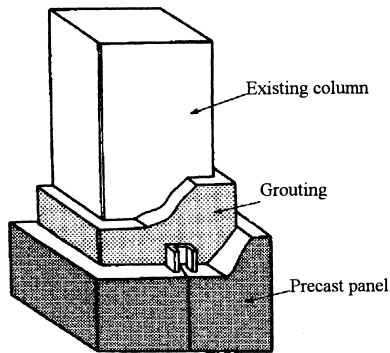


Fig. 15. Precast panel jacketing.

Table 5  
Design Earthquake Motions

| Levels of Earthquake Motion | Definitions  |
|-----------------------------|--|
| L1 motion                   | An earthquake motion which has a probability to occur a few times during the design lifetime of a structure                        |
| L2 motion                   | An earthquake motion which has small probability of occurrence during the design lifetime of structure but is very large intensity |

On the other hand, Level-2 (L2) Earthquake Motion is thought to be determined by fault investigations. Three kinds of response spectra, however, are set to express the Level-2 Earthquake Motion as shown in Table 6.

The L2 Spectrum-I is the minimum earthquake motion required to be taken into account in design. It covers not only earthquakes of magnitude 8 class, which occur at the plate boundaries, but also ones of magnitude 6.5 class, which occur at inland faults that are quite difficult to be detected. The L2 Spectrum-II is determined using 90% nonexcess probability curve resulting from 22 earthquake records. The maximum acceleration response value is set as  $1700 \text{ cm/s}^2$ . Seismic waves to fit these response spectra are also prepared.

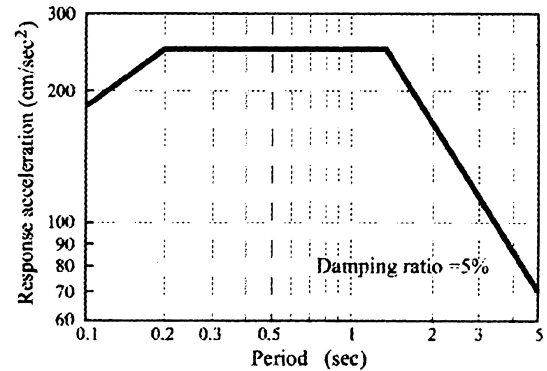


Fig. 16. Response spectrum of L1 motion.

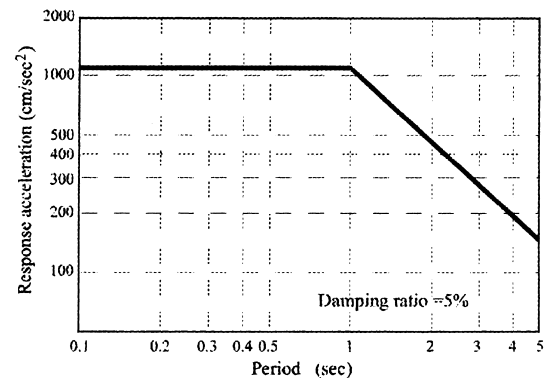


Fig. 17. Acceleration response spectrum for L2 motion (Spectrum-I).

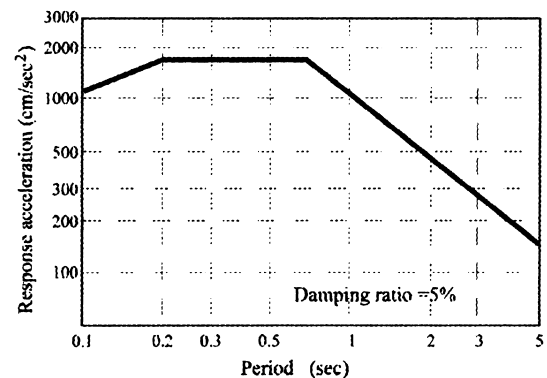


Fig. 18. Acceleration response spectrum for L2 motion (Spectrum-II).

To take into account the effect of surface ground, eight different ground profiles are determined according to their natural periods.

Inelastic dynamic time-domain analyses are adopted as the regular calculation method for design. However, the application of inelastic response spectra is allowed for the structure of which the first vibration mode is dominant to obtain required horizontal strength.

Table 6  
L2 response spectra

| Response spectra | Definitions   |
|------------------|---|
| I                | Elastic acceleration response spectrum to cover the earthquakes occur at plate boundaries   |
| II               | Elastic acceleration response spectrum determined using a statistical analysis on earthquake records collected from the inland type earthquakes |
| III              | Elastic acceleration response spectrum calculated by fault analysis   |

#### 4.3. Seismic performance of structure

Seismic performances of structures are classified into three categories depending on the preserved structural functions after the design assumed earthquakes as shown in Table 7. The basic requirement is that all structures shall satisfy Seismic Performance-I against L1 Earthquake Motion and Seismic Performance-II or -III against L2 Earthquake Motion.

Damages of members are also classified corresponding to the seismic performances of structures. Four categories of damage level are assigned as shown in Table 8 and they are correlated to the horizontal load–displacement relation as shown in Fig. 19.

The relation between the seismic performance of a structure and the damage level of a member basically depends on the structural type and function of the member. General relations, however, are indicated as follows: Damage Level 1 is assigned to the Seismic Performance-I. Damage Levels 2 and 3 are assigned to the Seismic Performance-II. Damage Levels 3 and 4 are assigned to the Seismic Performance-III.

The rotations of members to give the specified damage levels are shown in Table 9. They were derived based

Table 7  
Seismic performances of structures

| Seismic Performances | Definitions   | Earthquake to be checked |
|----------------------|---|--------------------------|
| I                    | Structure can sustain the original function without restoration work after earthquake and no excessive displacement occurs. | L1 motion                |
| II                   | Restoration work is necessary but the function of structure is recovered within a short period                              | L2 motion                |
| III                  | Structure system will not be collapsed by earthquake  |                          |

Table 8  
Damage levels of members

| Damage levels | Definitions   |
|---------------|---|
| 1             | No damage   |
| 2             | Repair work may be necessary according to conditions  |
| 3             | Repair work is necessary  |
| 4             | Repair work is necessary and replacement of member may be necessary according to conditions |

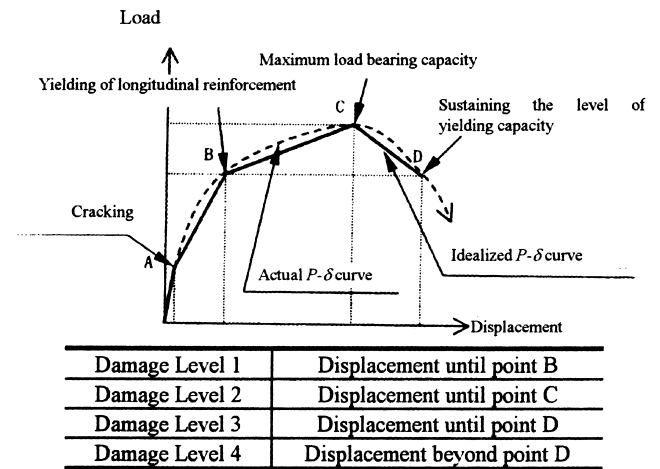


Fig. 19. Relation of damage level and  $P$ – $\delta$  curve.

on cyclic loading tests of RC columns. These rotations are verified with those calculated by dynamic response analysis as Eq. (20) in design.

$$\gamma_i \theta_d / \theta_{rd} \leq 1.0, \quad (20)$$

where,  $\gamma_i$  is the structure factor,  $\theta_d$  is the maximum rotation calculated by response analysis, and  $\theta_{rd}$  is the design rotation to give specified damage level.

By using the inelastic dynamic response analysis against L1 and L2 Earthquake Motions, which are determined based on the experience of Hyogoken-Nanbu Earthquake, and the design rotation capacities, a rational and practical seismic design for new railway concrete structure became possible.

#### 5. Concluding remarks

Outlines of restoration method of damaged structures in the Hyogoken-Nanbu Earthquake, popular seismic strengthening methods and their research backgrounds, and the concept of new seismic design standards for Japanese railway structures were presented.

Table 9  
Rotations of members to give specified damage levels

| Damage level   | Rotations of members to give specified damage levels (rotation capacities)   |
|----------------|--|
| Damage Level 1 | $\theta_y = \frac{\delta_{y0}}{l_a} + \theta_{y1} \quad (16)$ <p> <math>\delta_{y0}</math>: Displacement of member at Damage Level 1 (calculated using moment–curvature relations of RC member)<br/> <math>\theta_{y1}</math>: Rotation due to pull-out of longitudinal reinforcement at Damage Level 1<br/> <math>l_a</math>: Shear span </p>   |
| Damage Level 2 | $\theta_m = \frac{\delta_{mb} + \theta_{pm}(l_a - (h/2))}{l_a} + \theta_{m1} \quad (17)$ $\theta_{pm} = \frac{0.032K_{w0}p_w + 0.013}{0.79p_t + 0.153} \quad (18)$ <p> <math>\delta_{mb}</math>: Displacement of member except plastic hinge region at Damage Level 2 (calculated using moment–curvature relations of RC member)<br/> <math>\theta_{m1}</math>: Rotation due to pull-out of longitudinal reinforcement at Damage Level 2<br/> <math>K_{w0}</math>: Coefficient of hoop strength, <math>p_w</math>: hoop reinforcement ratio, <math>p_t</math>: longitudinal reinforcement ratio, <math>h</math>: section height </p> |
| Damage Level 3 | $\theta_n = \frac{\delta_{nb} + \{\theta_{pm} - (0.1/M_u)(M_y - M_u)\}(l_a - (h/2))}{l_a} + \theta_{n1} \quad (19)$ <p> <math>\theta_{n1}</math>: Rotation due to pull-out of longitudinal reinforcement at Damage Level 3<br/> <math>M_y</math>: Yielding flexural capacity, <math>M_u</math>: Flexural capacity </p>   |

We had very sorrowful experience in the Hyogoken-Nanbu Earthquake but we hope what we learned or studied from the experience contributes to the progress in seismic design of structures and to construct much safer facilities for the future.

## References

- [1] Yamamoto R, Fukada Y, Ueyama K, Tatsumi M, Oishibashi H. Gas pressure welding method for steel reinforcing bars. *Welding Journal* 1998;78(2):188-s–92-s.
- [2] Ministry of Transportation Notification, Urgent Actions for Seismic Strengthening on Existing Railway Structures, Railway Technical Division, No. 116, July 1995 (in Japanese).
- [3] Railway Technical Research Institute, Design Standards for Railway Concrete Structures and Commentary, October 1992 (in Japanese).
- [4] Railway Technical Research Institute, Design and Construction Guidelines for Seismic Strengthening on Railway Viaduct Columns using Carbon Fiber Sheets, July 1995 (in Japanese).
- [5] Railway Technical Research Institute, Design and Construction Guidelines for Seismic Strengthening on Railway Viaduct Columns using Aramid Fiber Sheets, November 1995.
- [6] Railway Technical Research Institute, Seismic Design Standards for Railway Structures, Final Draft, December 1998.